·临床研究·

3D 打印技术辅助成人脊柱侧后凸畸形的术前规划及应用价值

蒋维利，牛国旗，周功，陈辉，刘涛，聂虎，刘路坦，李超，周乾坤
（蚌埠医学院第二附属医院脊柱外科，安徽 蚌埠 233040）

【摘要】目的：探讨 3D 打印技术在成人脊柱侧后凸畸形的术前规划及术中辅助操作的应用价值。**方法**：回顾性分析 2017 年 9 月至 2019 年 1 月收治的 12 例成人脊柱侧后凸畸形患者，其中男 3 例，女 9 例；年龄 21~63（47.67±13.32）岁；先天性脊柱侧后凸畸形 4 例，脊柱陈旧性结核伴后凸畸形 2 例，特发性脊柱侧后凸畸形 2 例，退变性脊柱侧后凸畸形 4 例。将患者脊柱 CT 断层扫描数据导入 Mimics17.0 软件中，建立脊柱三维模型，通过 3D 打印机制作脊柱模型，然后进行术前规划及模拟手术操作，分析其术后影像学参数的改善情况。所有患者随访时间 1 年以上，于手术前后及末次随访时测量侧凸 Cobb 角，最大后凸 Cobb 角，冠状面平衡（distance between C_7 plumbline and center sacral vertical line，C_7PL-CSVL）和矢状面平衡（sagittal vertical axis，SVA），骨盆参数等相关影像学参数，进一步评估其矫形效果。**结果**：12 例脊柱侧后凸畸形患者的脊柱矫形术在 1:1 脊柱模型的指导下，采用不同的截骨矫形内固定融合方式（其中 4 例畸形较重的患者采用椎弓根螺钉置钉导板辅助椎弓根螺钉置入）置钉及截骨矫形，效果良好，术中、术后无血管、神经、脊髓等重要组织结构损伤，无脑脊液漏、感染等并发症发生。术前侧凸 Cobb 角为（56.5±22.5）°，后凸 Cobb 角为（65.2±19.5）°，C_7PL-CSVL 为（45.8±16.9）mm，SVA 为（48.7±25.4）mm。术后 4 周侧凸 Cobb 角为（20.8±11.5）°，后凸 Cobb 角为（22.0±6.6）°，矫正率分别为（65.1±9.7）% 和（64.6±10.6）%；C_7PL-CSVL 为（22.3±8.9）mm，SVA 为（23.3±13.1）mm，均较术前明显改善。12 例患者均随访 1 年以上，平均（18.5±7.9）个月，末次随访时侧、后凸 Cobb 角分别为（22.2±10.8）° 和（23.6±7.7）°，C_7PL-CSVL 为（23.5±10.8）mm，SVA 为（24.7±12.5）mm，较术前差异均有统计学意义（P<0.05），末次随访较术后差异无统计学意义（P>0.05）。**结论**：3D 打印模型可直观清晰地显示成人脊柱侧后凸畸形的椎体形态结构以及其与邻近椎体、血管、神经的空间关系，为手术方案个体化制定提供了良好、直观的立体解剖结构观察。术前预模拟手术操作，确定手术内固定、融合节段及截骨矫形方式，可以为实际临床手术提供参考，并能提高手术的精确性及安全性。

【关键词】 3D 打印技术； 脊柱侧后凸畸形； 截骨术

中图分类号：R687

DOI：10.12200/j.issn.1003-0034.2020.02.002

开放科学（资源服务）标识码（OSID）：

基金项目：蚌埠医学院自然科学基金面上项目（编号：BYKY18153）；蚌埠医学院科研创新团队项目（编号：BYKC201911）
Fund program：Natural Science Foundation of Bengbu Medical College（No：BYKY18153）

通讯作者：牛国旗 E-mail：ssngq@163.com
Corresponding author：NIU Guo-qi E-mail：ssngq@163.com

rigid scoliosis[J]. Zhongguo Gu Shang/China J Orthop Trauma, 2020, 33(2): 106-110. Chinese with abstract in English.

[7] 楼宇梁，全仁夫，李伟，等. 超声骨刀在退变性脊柱后凸截骨中的应用[J]. 中国骨伤，2020，33(2)：144-148.
LOU YL, QUAN RF, LI W, et al. Application of ultrasonic bone knife in osteotomy of degenerative kyphosis[J]. Zhongguo Gu Shang/China J Orthop Trauma, 2020, 33(2): 144-148. Chinese with abstract in English.

[8] Lafage Virginie, Schwab Frank, Patel Ashish, et al. Pelvic tilt and truncal inclination: two key radiographic parameters in the setting of adults with spinal deformity[J]. Spine, 2009, 34: E599-606.

[9] Glassman Steven D, Bridwell Keith, Dimar John R, et al. The impact of positive sagittal balance in adult spinal deformity[J]. Spine, 2005, 30(18): 2024-2029.

[10] 邱勇，王斌，朱锋，等. 退变性腰椎侧凸的冠状面失衡分型及对截骨矫形术式选择的意义[J]. 中华骨科杂志，2009，29(5)：418-423.
QIU Y, WANG B, ZHU F, et al. Classification of coronal trunk unbalance in degenerative lumbar scoliosis and its influence on osteotomy strategy[J]. Zhonghua Gu Ke Za Zhi, 2009, 29(5): 418-423. Chinese.

[11] 蒋维利，牛国旗，周功，等. 3D 打印技术辅助成人脊柱侧后凸畸形的术前规划及临床疗效分析[J]. 中国骨伤，2020，33(2)：99-105.
JIANG WL, NIU GQ, ZHOU G, et al. 3D printing technology assisted the preoperative planning and application value in adult kyphoscoliosis deformity[J]. Zhongguo Gu Shang/China J Orthop Trauma, 2020, 33(2): 99-105. Chinese with abstract in English.

（收稿日期：2020-02-07 本文编辑：王宏）

3D printing technology assisted the preoperative planning and application value in adult kyphoscoliosis deformity

JIANG Wei-li, NIU Guo-qi, ZHOU Gong, CHEN Hui, LIU Tao, NIE Hu, LIU Lu-tan, LI Chao, and ZHOU Qian-kun. Department of Spinal Surgery, the Second Affiliated Hospital of Bengbu Medical College, Bengbu 233040, *Anhui, China*

ABSTRACT **Objective**: To explore the application value of 3D printing technology in preoperative surgery plan and intraoperative auxiliary operation for adult kyphoscoliosis deformity. **Methods**: The clinical data of 12 adult patients with kyphoscoliosis deformity treated from September 2017 to January 2019 were retrospectively analyzed. There were 3 males and 9 females, aged from 21 to 63 years old with an average of (47.67±13.32) years old. Among them, 4 cases were congenital kyphoscoliosis, 2 cases were old tuberculosis thoracolumbar kyphosis; 2 cases were idiopathic kyphoscoliosis, 4 cases were degenerative kyphoscoliosis. The CT scan data of the patient´s spine was imported into Mimics17.0 software to establish the three-dimensional model of the spine, and the spine model was produced by 3D printer. Using the spine model simulated operation, preoperative surgery program planning and formulated a precise surgery, and further analysed postoperative imaging parameters improvement. All the patients were followed up for more than 1 year. Before and after operation and at the last follow-up, the scoliosis Cobb angle, maximum kyphosis Cobb angle, and coronal plane balance (distance between C_7 plumbline and center sacral vertical line, C_7PL-CSVL), sagittal plane balance (sagittal vertical axis, SVA), pelvic parameters and other related imaging parameters were measured to further evaluate its orthopedic effect. **Results**: Twelve patients with spine deformity were treated with different osteotomy and internal fixation fusion methods under the guidance of a 1:1 spine model (pedicle screw placement of 4 patients with severe deformity were assisted by pedicle screw guide plates), nail placement and osteotomy have good effects, no major tissue damage such as blood vessels, nerves and spinal cord during and after surgery, no complications such as cerebrospinal fluid leakage and infection. Preoperative Cobb angle of scoliosis was (56.5±22.5)°, Cobb angle of kyphosis was (65.2±19.5)°, C_7PL-CSVL was (45.8±16.9) mm, SVA was (48.7±25.4) mm. Postoperative at 4 weeks, Cobb angle of scoliosis was (20.8±11.5)°, and Cobb angle of kyphosis was (22.0±6.6)°, with correction rates of (65.1±9.7)% and (64.6±10.6)%, respectively; C_7PL-CSVL was (22.3±8.9) mm, and SVA was (23.3±13.1) mm, all of which were significantly improved compared with preoperative results. The mean follow-up time was (18.5±7.9) months in 12 patients. At the last follow-up, the Cobb angles of scoliosis and kyphosis were (22.2±10.8)° and (23.6±7.7)°, respectively, C_7PL-CSVL was (23.5±10.8) mm, and SVA was (24.7±12.5) mm. The results were statistically significant compared preoperative ($P<0.05$). There was no significant difference at the postoperative at 4 weeks and the last follow-up ($P>0.05$). **Conclusion**: The 3D print model can visually and clearly show the vertebral morphology and structure of adult kyphoscolisis and its spatial relationship with the adjacent vertebrae, blood vessels, and nerves, which provides a good and intuitive stereoscopic anatomical structure observation for the individualization of the surgical plan. Pre-simulation of operations to determine the internal fixation, fusion segment and osteotomy orthopedic way, may to provide a reference for actual clinical surgery, and can improve the accuracy and safety of surgery.

KEYWORDS 3D printing technology; Kyphoscoliosis deformity; Osteotomy

近年来随着 3D 打印技术在各行各业的不断发展，在医学众多领域中的应用也极为广泛[1-4]。该技术可以使临床医生在术前充分认识手术区域内的详细情况，并进行合理的术前设计，术中严格遵循既定的术前规划，提高手术的精确性，缩短手术时间，提高手术的安全性及手术质量。而且已经在骨肿瘤切除、骨盆骨折、关节置换、脊柱外科等方面有了很好的临床及科研方面的应用[5-8]。但是 3D 打印技术在成人脊柱侧后凸畸形患者的术前规划应用报道较少，本研究通过选取成人脊柱侧后凸畸形患者，利用 3D 打印技术个体化和精准化特点，打印 3D 脊柱模型用于术前规划，确定手术内固定融合、减压及截骨矫形的节段及范围，探讨其临床应用价值，报告如下。

1 资料与方法

1.1 病例选择

纳入标准：所有脊柱侧后凸畸形患者均为成年人；脊柱侧后凸畸形临床症状明显且需要手术治疗的患者；无明显手术禁忌证；签署知情同意书且临床资料完整；随访时间达 1 年以上。

排除标准：患有严重基础疾病不能耐受手术患者；脊柱侧后凸畸形不严重可以保守治疗的患者；其他不明原因导致的脊柱侧后凸畸形患者；临床资料不完整患者。

1.2 一般资料

按照上述病例选择标准，收集 2017 年 9 月至 2019 年 1 月成人脊柱侧后凸畸形患者 12 例，其中男 3 例，女 9 例；年龄 21~63(47.67±13.32)岁；先天性脊柱侧后凸畸形 4 例，脊柱陈旧性结核伴后凸畸形 2 例，特发性脊柱侧后凸畸形 2 例，退变性脊柱侧后凸畸形 4 例。

1.3 研究方法

1.3.1 数据采集及处理 12 例患者手术前后均行站立位脊柱全长正侧位 X 线，左右 Bending 位像，胸腰椎正侧位 X 线，三维 CT 扫描(荷兰，Philips 公司)

检查，将 CT 连续断层图像数据以 DICOM 格式保存。将获取的 CT 数据导入可自动检测、识别 DICOM 格式文件的医学三维重建 Mimics 17.0（比利时，Materialise 公司）软件中，将数据转化成三维图像。

1.3.2　脊柱模型的建立　将 12 例患者的脊柱 64 排螺旋 CT 连续断层扫描数据以 DICOM 格式保存，输入计算机，运用医学三维重建软件 Mimics 17.0 对 CT 连续断层扫描数据进行处理。Mimics 17.0 软件直接利用 CT 断层原始数据格式，无须图像转换，减少了格式转换过程中出现的信息丢失。运用相应软件对骨组织及软组织进行分割处理，根据需要选取需要重建的脊柱节段，便可重建出所需的脊柱骨骼模型，并根据脊柱矢状位与冠状位平衡模拟脊柱畸形截骨矫形术。然后将重建的脊柱模型以 STL 格式导出，并导入 Idea Maker 软件，利用此软件进行切片，再导入打印机（Raise3D N2Plus）进行模型打印，计算机脊柱模型的建立流程图见图 1。

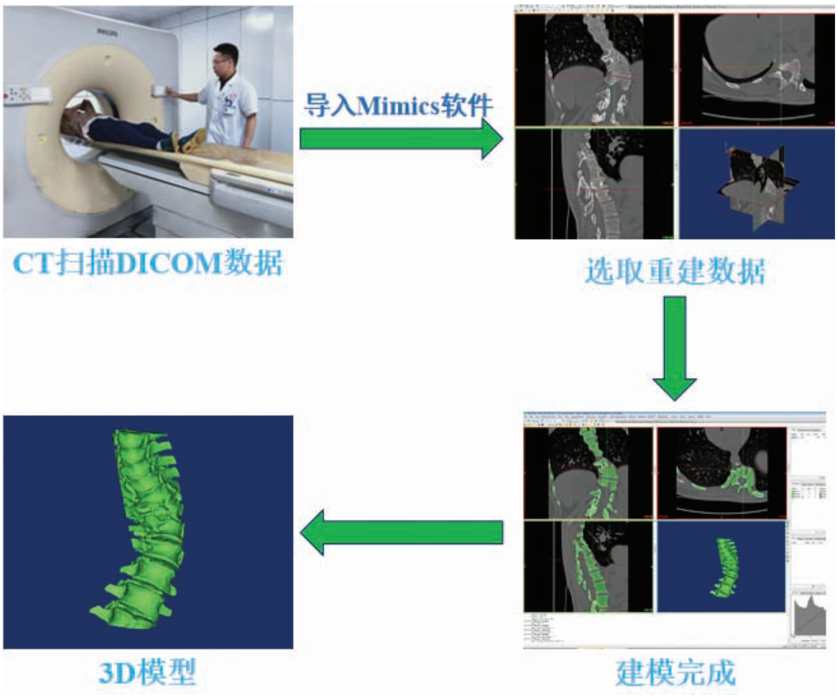

图 1　计算机脊柱模型的建立流程图
Fig.1　Flowchart of the establishment of the computer spinal model

1.3.3　术前规划及模拟手术　预先在 Mimics 软件上设计截骨平面和节段，进行预模拟截骨，观察模拟截骨后的矫形效果，最后在 3D 打印脊柱模型上进行体外模拟截骨矫形"手术"，最终为实际术中截骨矫形提供精准参考。仔细观察模型形态，根据患者不同的畸形特点制定个体化手术方案，可在术前模拟手术方案，包括规划内固定融合节段、螺钉置入位置和方向、截骨矫形术式选择与范围确定等手术操作（图 2）。

1.3.4　实际临床手术　采用 3D 打印技术将脊柱畸形模型打印出来，预先设计出具体的手术方案，其中包括内固定融合节段、螺钉置入位置和方向、椎体截骨的方式及截骨的范围等，并将模型予以等离子消毒后供术中截骨矫形参考。术中采用神经电生理监护仪监护患者神经功能，根据术前规划方案采用超声骨刀进行截骨矫形。

1.4　观察项目与方法

记录 12 例患者手术前后及随访 1 年以上时相关临床评估指标。

影像学评估包括：（1）侧凸 Cobb 角，站立位全脊柱正位像 X 线片上测量主弯上下端椎之间的侧凸角度。（2）最大后凸 Cobb 角（global kyphosis，GK），站立位全脊柱侧位像 X 线片上测量顶椎最倾斜椎体的上终板与下端椎最倾斜椎体下终板切线之间夹角。（3）冠状面平衡（C_7PL-CSVL），站立位全脊柱正位 X 线片上测量 C_7 铅垂线（C_7 plumb line，C_7PL）至

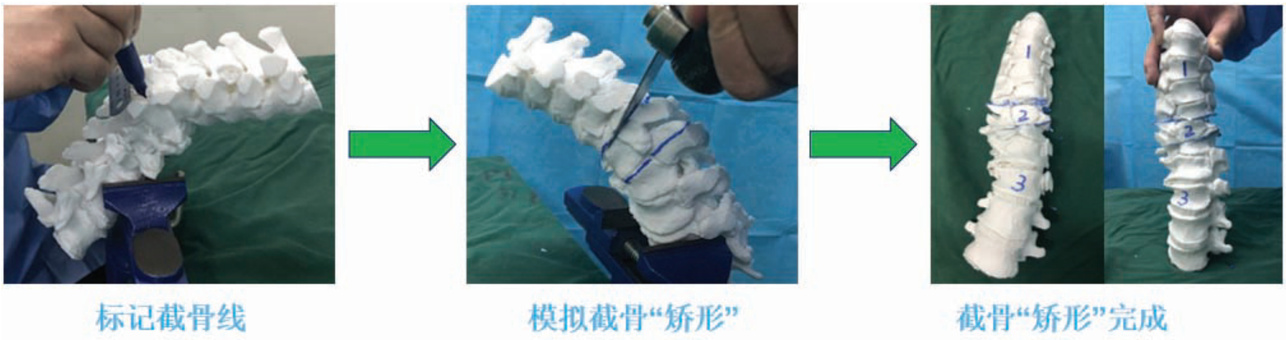

图 2　脊柱矫形的术前规划及模拟手术过程
Fig.2　Preoperative planning and simulation of spinal orthopedics

骶骨中垂线（center sacral vertical line，CSVL）的距离。(4)矢状面平衡(sagittal vertical axis，SVA)，站立位全脊柱侧位 X 线片上测量 C_7 铅垂线与骶骨后上角的水平距离，C_7 铅垂线在骶骨后上角前方为正、后方为负。

详细记录患者术中及术后的并发症，评估有无血管神经损伤、有无伤口感染、不愈合、矫形效果不佳、椎弓根螺钉位置不佳、内固定失效等。

1.5　统计学处理

采用 SPSS 18.0 统计软件进行数据处理，手术前后的影像学数据定量资料以均数±标准差（$\bar{x}\pm s$）表示，采用配对 t 检验，以 $P<0.05$ 为差异有统计学意义。

2　结果

12 例患者的脊柱矫形术在 1∶1 脊柱模型的指导下，采用后入路不同的截骨矫形内固定融合方式，术中准确、快速的暴露出畸形椎体的解剖位置，清晰的观察到畸形椎体的解剖空间形态，避免了术中置钉和截骨操作对神经、血管及脊髓损伤，置钉及截骨效果均满意，截骨矫形效果良好，术中和术后无血管、神经、脊髓等重要组织结构损伤，无脑脊液漏、感染、螺钉位置不佳、内固定失效等并发症发生。根据模拟矫形方案实际手术截骨方式见表 1，实际置入螺钉数目 8~19(13.7±3.1)个。

12 例患者术前侧凸 Cobb 角为(56.5±22.5)°；后凸 Cobb 角为（65.2±19.5）°；C_7PL-CSVL 为（45.8±16.9）mm；SVA 为(48.7±25.4)mm。术后 4 周侧凸 Cobb 角为(20.8±11.5)°，后凸 Cobb 角为(22.0±6.6)°，矫正率分别为(65.1±9.7)%和(64.6±10.6)%；C_7PL-CSVL 为(22.3±8.9) mm，SVA 为(23.3±13.1)mm，均较术前明显改善。12 例患者均随访 1 年以上，平均随访时间(18.5±7.9)个月，末次随访时侧、后凸 Cobb 角分别为(22.2±10.8)°和(23.6±7.7)°，C_7PL-CSVL 为(23.5±10.8) mm，SVA 为(24.7±12.5) mm，与术前比较，差异均有统计学意义($P<0.05$)，末次随访与术后 4 周比较差异无统计学意义($P>0.05$)。见表 2。典型病例见图 3。

3　讨论

随着科学技术的迅速发展，数字化技术的应用已经在医学的各个领域找到生存空间，特别是外科手术正在向个体化、精准化、微创化发展，数字化骨科技术已经成为现代医学一个新的领域[9-11]，如计算机辅助影像导航骨科手术可以在骨科手术方面实现更加微创、更加智能的手术方式[12-17]。而 3D 打印技术也逐渐在骨科领域被推广和运用，该技术以模型数据为基础，将材料速溶后按指定顺序逐层堆积成形。目前，应用 3D 打印技术进行术前规划已经成为一种骨科发展趋势，在各种骨科手术如脊柱手术、四肢肿瘤手术、关节置换手术、四肢骨折及骨盆骨折内固定手术中均有很好的临床实验研究及运用[5,18-22]，并取得了较好的临床疗效，但在成人脊柱侧后凸畸形术前规划的报道还很少[23-24]。

成人脊柱后凸畸形临床并不少见，常发生于陈旧性创伤、陈旧性结核、脊柱先天性畸形等。中-重度脊柱侧后凸畸形常常伴有不同程度的胸腰背痛和下

表 1　脊柱侧后凸畸形 12 例患者的一般资料及手术情况

Tab.1　General data and operative information of 12 patients with kyphoscoliosis deformity

编号	性别	年龄(岁)	诊断	截骨节段	截骨方式	固定节段	置入螺钉数(枚)	手术入路
1	女	50	TK	T_{12},L_1	多节段 PSO	T_8-L_4	15	后路
2	女	41	CS	T_8,T_9	VCR、PSO	T_3-L_4	19	后路
3	男	21	IS	L_3	VCR	T_{11}-L_5	12	后路
4	男	44	DS	T_{10}-L_1	多节段 SPO	T_{10}-L_5	14	后路
5	女	48	CS	T_{10}-L_1	PSO	T_{10}-L_5	14	后路
6	女	25	IS	T_7-T_{10}	多节段 SPO	T_6-L_4	14	后路
7	男	63	DS	T_{10}-L_1	多节段 SPO	T_{10}-L_5	16	后路
8	女	51	CS	T_{12}	PSO	T_{11}-L_4	10	后路
9	女	62	DS	L_3-L_5	多节段 SPO	L_3-S_1	8	后路
10	女	59	CS	L_3	PSO	T_9-L_5	17	后路
11	女	53	DS	T_{10}-L_1	多节段 SPO	T_{10}-L_5	14	后路
12	女	55	TK	L_4	VCR	T_{12}-I	11	后路

注：IS，特发性脊柱侧凸；CS，先天性脊柱侧凸；TS，陈旧性结核胸腰椎后凸；DS，退变性脊柱侧凸；SPO，Smith-Petersen 截骨；PSO，经椎弓根椎体截骨术；VCR，全椎体切除截骨术；T，胸椎；L，腰椎；S，骶椎；I，髂骨

Note：IS，idiopathic scoliosis；CS，congenital scoliosis；TK，tuberculosis kyphosis；DS，degenerative scoliosis；SPO，Smith-Petersen osteotomy，PSO，pedicle subtraction osteotomy；VCR，vertebral column resection；T，thoracic；L，lumbar；S，sacral；I，ilium

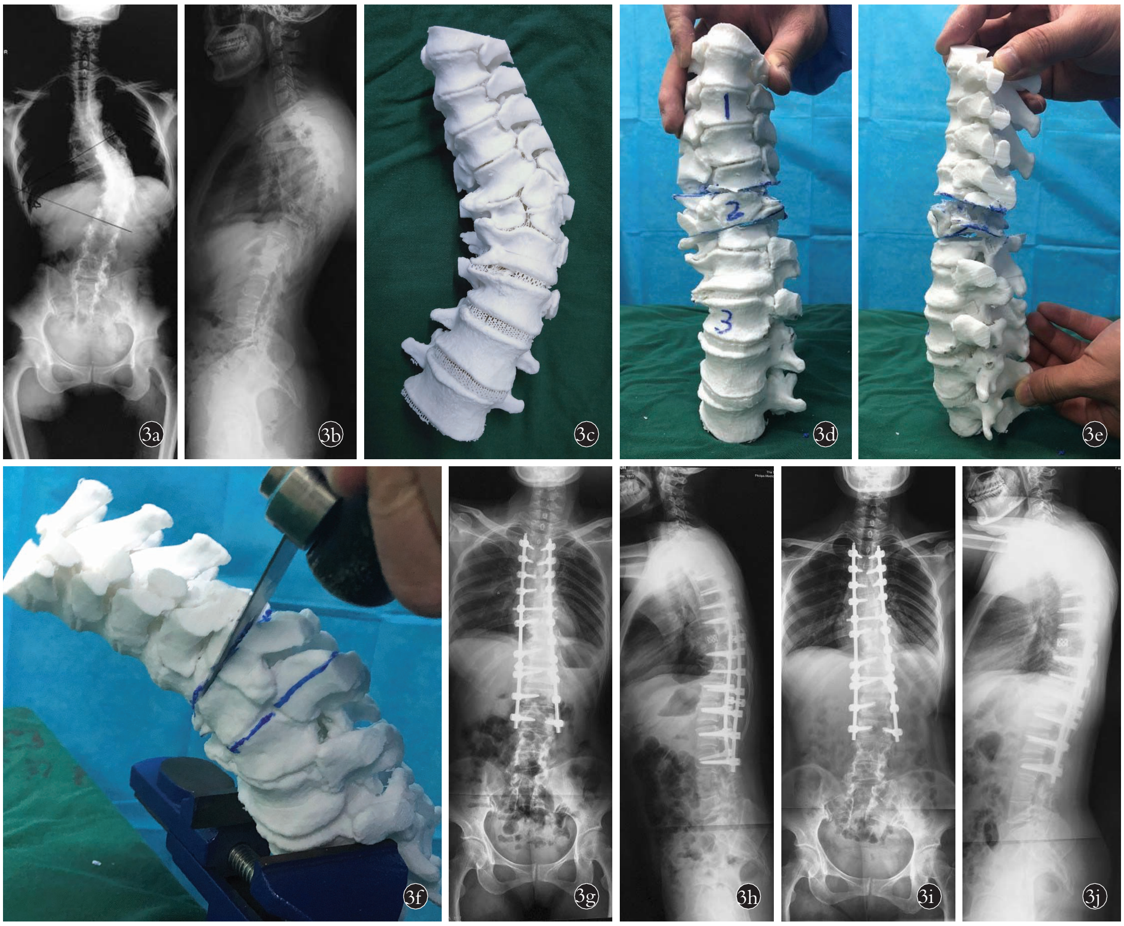

图 3　女性患者，41 岁，因"自幼脊柱畸形伴胸背部疼痛不适 30 余年"入院。诊断：先天性脊柱侧后凸畸形　**3a，3b.** 术前站立位全脊柱正侧位 X 线片，胸椎最大侧凸 Cobb 角为 49°，最大后凸 Cobb 角为 70°　**3c，3d，3e，3f.** 术前规划截骨矫形术。通过颈椎三维 CT 打印出 1∶1 畸形的脊柱模型，仔细观察模型形态，与影像学对比，并进行术前手术模拟。即行后路切开胸腰椎截骨矫形融合内固定术，术中见后凸畸形部位、形态及其与周围结构解剖关系与打印模型一致，按照术前模拟操作快速行椎弓根螺钉置入及截骨矫形手术，并予以植骨融合钉棒内固定　**3g，3h.** 术后 1 个月站立位全脊柱正侧位 X 线片，胸椎最大侧凸 Cobb 角矫正到术后 7°，最大后凸 Cobb 角矫正到术后 30°　**3i，3j.** 术后 1.5 年站立位全脊柱正侧位 X 线片，胸椎最大侧凸 Cobb 角为 8°，最大后凸 Cobb 角为 36°

Fig.3　Female patient, 41 years old, was admitted to the hospital for "more than 30 years since childhood spinal deformity with chest and back pain and discomfort", and was diagnosed as congenital kyphoscoliosis deformity　**3a, 3b.** Preoperative standing total spinal X-rays showed the maximum scoliosis Cobb angle was 49° and the maximum kyphosis Cobb angle was 70°　**3c, 3d, 3e, 3f.** Preoperative planning for osteotomy and orthopedics. A 1∶1 deformed spinal model was printed by three-dimensional CT of the cervical spine, and the shape of the model was carefully observed, compared with imaging, and preoperative surgical simulation was performed. The posterior thoracolumbar osteotomy and orthopedic fusion were performed, and the kyphosis position, shape and the anatomical relationship with the surrounding structure were consistent with the printed model. Pedicle screw placement and the location and scope of osteotomy and orthopedic were performed quickly according to the preoperative simulation, and internal fixation was performed with bone graft fusion and screw rod　**3g, 3h.** One month postoperatively, standing total lateral spine X-rays showed the maximum scoliosis Cobb angle was corrected to 8°, and the maximum kyphosis Cobb angle was corrected to 36°　**3i, 3j.** One year and 6 months postoperatively, standing total lateral spine X-rays showed the maximum scoliosis Cobb angle was 8°, and the maximum kyphosis Cobb angle was 36°

肢神经症状，多需要手术治疗，而重度脊柱侧后凸多指冠状面 Cobb 角>80°，左右 Bending 像脊柱柔韧性<30%。重度脊柱畸形患者在接受手术治疗时具有以下特点：受累脊柱节段的柔韧度明显降低，头尾侧代偿弯多演变为结构性弯，且常伴有躯干的严重失衡，较难获得满意矫形；原发的椎体发育畸形或继发的椎体过度旋转及代偿的骨性增生使得矫形器械置入困难；此类患者由于侧后凸局部畸形重，解剖关系复杂，截骨难度高，手术风险较高，并发症发生率高，一直为脊柱外科领域的难点[25-27]。近年来随着脊柱截骨技巧和内固定技术的迅速发展，单纯后路脊柱截骨矫形手术临床上应用最广，然而值得注意的是，成人脊柱侧后凸畸形的矫形手术风险仍较高，可能出现的并发症包括脑脊液漏、血管损伤、神经根损伤、脊髓损伤和内固定失败等[28-29]，故仍然是临床脊柱外科医生具挑战性的高难度手术。

表2 手术前后12例脊柱侧后凸畸形患者的影像学参数评估结果($\bar{x}\pm s$)

Tab.2 Measurement results of imaging parameters of 12 patients with kyphoscoliosis deformity before and after operation($\bar{x}\pm s$)

项目	术前	术后4周	末次随访
侧凸 Cobb 角(°)	56.5±22.5	20.8±11.5○	22.2±10.8●
后凸 Cobb 角(°)	65.2±19.5	22.0±6.6△	23.6±7.7▲
C_7PL–CSVL (mm)	45.8±16.9	22.3±8.9☆	23.5±10.8★
SVA (mm)	48.7±25.4	23.3±13.1◇	24.7±12.5◆

注:与术前比较,○t=10.062,P<0.001;△t=8.329,P<0.001;☆t=7.193,P<0.001;◇t=4.663,P<0.001.○与●比较,t=1.685,P=0.120。△与▲比较,t=1.345,P=0.206; ☆与★比较,t=0.884,P=0.395;◇与◆比较,t=0.983,P=0.347

Note:Compared with preoperative data,○t=10.062,P<0.001;△t=8.329,P<0.001;☆t=7.193,P<0.001;◇t=4.663,P<0.001.○vs●,t=1.685,P=0.120;△vs▲,t=1.345,P=0.206; ☆vs★,t=0.884,P=0.395;◇vs◆,t=0.983,P=0.347

3D打印成人脊柱侧后凸畸形脊柱模型数据是通过Mimics软件平台,利用镜像技术将畸形脊柱的三维重建数据进行处理,并预设计出截骨矫形后脊柱在矢状位及冠状位得到最佳平衡的手术方案,进一步个性化打印出患者畸形脊柱的3D实体模型,并在3D打印脊柱实体模型上进行截骨模拟手术,按照预设计手术方案应用于手术可提高螺钉置入及截骨精准度,缩短手术时间,降低脊髓损伤的风险,提高矫形效果等等。严重脊柱侧后凸畸形患者椎弓根螺钉的置钉点、置钉角度的确定也是手术的难点,根据1:1脊柱模型术前可确定椎弓根及关节突关节的位置,以及最佳椎弓根螺钉进钉点和螺钉置钉位置。本组采用3D打印技术辅助全脊柱模型设计手术内固定融合及截骨矫形方案,并运用到实际手术当中,作为参考进一步指导实际手术,优化手术程序,提高脊柱矢状位及冠状位矫形效果,降低并发症的发生率,具有极大的临床推广应用价值。此外,还可以术前设计椎弓根螺钉导板,借助椎弓根导板模型确定及提高置钉的精确性,最大化降低钉道打入椎管损伤脊髓的概率,间接提高手术安全性[30-32]。本组中有4例患者采用椎弓根导板技术,提高了术中螺钉置入准确率,节省了手术时间,降低了脊髓神经根损伤等并发症,进一步优化了手术效果。

综上所述,通过对成人脊柱侧后凸畸形患者采用术前3D打印技术,模拟内固定、融合节段,规划截骨方案进一步指导实际临床截骨矫形手术,使患者取得个性化的截骨手术方案,从而取得更好的矫形效果,术中可以精准的进行截骨矫形及有效的椎弓根螺钉置入,在一定程度上缩短了手术时间,减少了术中出血,降低了手术并发症,保障了患者手术的精确性及安全性。

参考文献

[1] Wasinpongwanich K, Paholpak P, Tuamsuk P, et al. Morphological study of subaxial cervical pedicles by using three-dimensional computed tomography reconstruction image[J]. Neurol Med Chir (Tokyo), 2014, 54(9): 736–745.

[2] 吴天琦,杨春喜. 可用于骨修复的3D打印多孔支架研究进展[J]. 中国修复重建外科杂志, 2016, 30(4): 509–513.
WU TQ, YANG CX. Research progress of three-dimensional printing porous scaffolds for bone tissue engineering[J]. Zhongguo Xiu Fu Chong Jian Wai Ke Za Zhi, 2016, 30(4): 509–513. Chinese.

[3] Dankowski R, Baszko A, Sutherland M, et al. 3D heart model printing for preparation of percutaneous structural interventions: description of the technology and case report[J]. Kardiol Pol, 2014, 72(6): 546–551.

[4] Wu AM, Lin JL, Kwan KYH, et al. 3D-printing techniques in spine surgery: the future prospects and current challenges[J]. Expert Rev Med Devices, 2018, 15(6): 399–401.

[5] 李涛,陈卓夫,龚辉,等. 3D打印技术在复杂髋臼骨折术中的初步临床应用[J]. 中国骨与关节损伤杂志, 2016, 31(4): 387–388.
LI T, CHEN ZF, GONG H, et al. Preliminary clinical application of 3D printing technology in complex acetabular fracture surgery[J]. Zhongguo Gu Yu Guan Jie Sun Shang Za Zhi, 2016, 31(4): 387–388. Chinese.

[6] Dankowski R, Baszko A, Sutherland M, et al. 3D heart model printing for preparation of percutaneous structural interventions: description of the technology and case report[J]. Kardiol Pol, 2014, 72(6): 546–551.

[7] Wu AM, Shao ZX, Wang JS, et al. The accuracy of a method for printing three-dimensional spinal models[J]. PLoS One, 2015, 10(4): e0124291.

[8] Chen H, Wu D, Yang H, et al. Clinical use of 3D printing guide plate in posterior lumbar pedicle screw fixation[J]. Med Sci Monit, 2015, 21: 3948–3954.

[9] Arai K, lwanaga S, Toda H, et al. Three-dimensional inkjet biofabrication based on designed images[J]. Biofabrication, 2011, 3(3): 034113.

[10] 庄怀铭,郭跃跃,林勇彬,等. 颈前路加压螺钉内固定治疗齿状突骨折的临床研究[J]. 中华全科医学, 2012, 10(7): 1063–1065.
ZHUANG HM, GUO YY, LIN YB, et al. Clinical analysis on cervical anterior compression screw for odontoid fracture[J]. Zhonghua Quan Ke Yi Xue, 2012, 10(7): 1063–1065. Chinese.

[11] 郝定均,贺宝荣,许正伟,等. 寰椎"椎弓根"三维CT重建测量及分型的临床意义[J]. 中国脊柱脊髓杂志, 2012, 22(2): 142–146.
HAI DJ, HE BR, XU ZW, et al. Clinical significance of measurements and classification of atlas pedicles by three-dimensional computer tomography and reconstruction[J]. Zhongguo Ji Zhu Ji Sui Za Zhi, 2012, 22(2): 142–146. Chinese.

[12] Attias N, Lindsey RW, Starr AJ, et al. The use of a virtual three-dimensional model to evaluate the intraosseous space available for percutaneous screw fixation of acetabular fractures[J]. J Bone

Joint Surg Br, 2011, 87(11): 1520–1523.

[13] Yoshiharu K, Masato N, Taketoshi Y, et al. Development of a new technique for pedicle screw and Magerl screw insertion using a 3-dimensional image guide[J]. Spine(Phila Pa 1976), 2012, 37(23): 1983–1988.

[14] Ma T, Xu YQ, Cheng YB, et al. A novel computer assisted drill guide template for thoracic pedicle screw placement: a cadaveric study[J]. Arch Orthop Trauma Surg, 2012, 1: 65–72.

[15] Sugawara T, Higashiyama N, Kaneyama S, et al.Multistep pedicle screw insertion procedure with patient specific lamina fit-and-lock templates for the thoracic spine: clinical article[J]. J Neurosurg Spine, 2013, 2: 185–190.

[16] Merc M, Drstvensek I, Vogrin M, et al.A multi-level rapid prototyping drill guide template reduces the perforation risk of pedicle screw placement in the lumbar and sacral spine[J]. Arch Orthop Trauma Surg, 2013, 7: 893–899.

[17] Merc M, Drstvensek I, Vogrin M, et al. Error rate of multi-level rapid prototyping trajectories for pedicle screw placement in lumbar andsacral spine[J]. Chin J Traumatol, 2014, 5: 261–266.

[18] 马立敏, 张余, 周烨, 等. 3D 打印技术在股骨远端骨肿瘤的应用[J]. 中国数字医学 2013, 8(8): 70–72.
MA LM, ZHANG Y, ZHOU Y, et al. Application of 3D printing technology in the treatment of distal femur bone tumor[J]. Zhongguo Shu Zi Yi Xue, 2013, 8(8): 70–72. Chinese.

[19] 吴东迎, 袁峰, 吴继彬, 等. 3D 打印截骨导板在人工全膝关节置换术中的应用[J]. 中华骨科杂志, 2015, 35(9): 921–926.
WU DY, YUAN F, WU JB, et al. Clinical application of 3D printing guild plate in total knee arthroplasty[J]. Zhonghua Gu Ke Za Zhi, 2015, 35(9): 921–926. Chinese.

[20] 邱冰, 唐本森, 邓必勇, 等. 基于三维反求技术和计算机辅助技术的 3D 打印导板在全膝关节置换术中的初步应用[J]. 中华创伤骨科杂志, 2016, 18(1): 35–41.
QIU B, TANG BS, DENG BY, Liu F, et al. Intelligentized surgery based on 3D printing technology for personalized total knee arthroplasty[J]. Zhonghua Chuang Shang Gu Ke Za Zhi, 2016, 18(1): 35–41. Chinese.

[21] Lee JY, Lee JW, Pang KM, et al. Biomechanical evaluation of magnesium-based resorbable metallic screw system in a bilateral sagittal split ramus osteotomy model using three-dimensional finite element analysis[J]. J Oral Maxillofac Surg, 2014, 72(2): 402.e1–13.

[22] Yang M, Zeng C, Guo S, et al. Digitalized design of extraforaminal lumbar interbody fusion: a computer-based simulation and cadaveric study[J]. PLoS One, 2014, 9(8): e105646.

[23] Illés T, Somoskeöy S. Comparison of scoliosis measurements based on three-dimensional vertebra vectors and conventional two-dimensional measurements: advantages in evaluation of prognosis and surgical results[J]. Eur Spine J, 2013, 22(6): 1255–1263.

[24] Fu J, Liu C, Zhang YG, et al. Three-dimensional computed tomography for assessing lung morphology in adolescent idiopathic scoliosis following posterior spinal fusion surgery[J]. Orthop Surg, 2015, 7(1): 43–49.

[25] Suk SI, Kim JH, Lee SM, et al. Anterior-posterior surgery versus posterior closing wedge osteotomy in posttraumatic kyphosis with neurologic compromised osteoporotic fracture[J]. Spine (Phila Pa 1976), 2003, 28(18): 2170–2175.

[26] Qian BP, Qiu Y, Wang B, et al. Pedicle subtraction osteotomy through pseudarthrosis to correct thoracolumbar kyphotic deformity in advanced ankylosing spondylitis[J]. Eur Spine J, 2012, 21(4): 711–718.

[27] Arun R, Dabke HV, Mehdian H. Comparison of three types of lumbar osteotomy for ankylosing spondylitis: a case series and evolution of a safe technique for instrumented reduction[J]. Eur Spine J, 2011, 20(12): 2252–2260.

[29] 曾岩, 陈仲强, 郭昭庆, 等. 中–重度脊柱后凸成角畸形后路矫形手术的并发症及其对策[J]. 中国脊柱脊髓杂志, 2011, 21(6): 468–473.
ZENG Y, CHEN ZQ, GUO ZQ, et al. The complications and management of posterior correction for moderate/severe kyphosis[J]. Zhongguo Ji Zhu Ji Sui Za Zhi, 2011, 21(6): 468–473. Chinese.

[29] Blondel B, Schwab F, Bess S, et al. Posterior global malalignment after osteotomy for sagittal plane deformity: it happens and here is why[J]. Spine(Phila Pa 1976), 2013, 38(7): E394–401.

[30] Guarino J, Tennyson S, McCain G, et al. Rapid prototyping technology for surgeries of the pediatric and pelvis: benefits analysis[J].J Pediatr Orthop, 2000, 27(8): 955–960.

[31] Merc M, Igor D, Vogrin M, et al. Amulti-level rapid prototyping drill guide template reduces the perforation risk of pedicle screw placement in the lumbar and sacral spine[J]. Arch Orthop Traum Surg, 2013, 133: 893–899.

[32] Wu ZX, Huang LY, Sang HX, et al. Accuracy and safety assessment of pedicle screw placement using the rapid prototyping technique in severe congenital scoliosis[J]. J Spinal Disord Tech, 2011, 24(7): 444–450.

(收稿日期: 2019–12–08 本文编辑: 王宏)